New AME Sources with the QUIJOTE MFI

Frédérick Poidevin on behalf of the QUIJOTE team

CMB foregrounds for B-mode studies

Tenerife, October 15-18 2018

RADIO FOREGROUNDS

H2020 – G.A. 687312

Plan of the Talk:

1) Observations and data sample
2) QUIJOTE-MFI intensity maps
3) SED Fitting
4) SEDs in intensity
5) Comparisons with Planck IR XV (2014)
6) Results of our analysis
7) Summary

1) Observations and data sample

- LFI maps:
  - Haslam (0.4 GHz),
  - Dwingeloo (0.8 GHz)
  - Reich (1.42 GHz)
  - HartRao (2.326 GHz).
- Maps at 11, 13, 17 and 19 GHz are from the QUIJOTE-MFI wide-survey (See José Alberto Rubiño-Martín's talk).
- WMAP 9-year maps.
- Planck PR2 I maps and PR3 Q and U maps
- Dirbe maps

1) Observations and data sample

- Data sample: 51 AME candidates of PIR XV (2014) have been observed with the QUIJOTE-MFI
- 12 sources of interest (mainly molecular cloud regions) point-sources like have been added to the final sample of 63 sources.

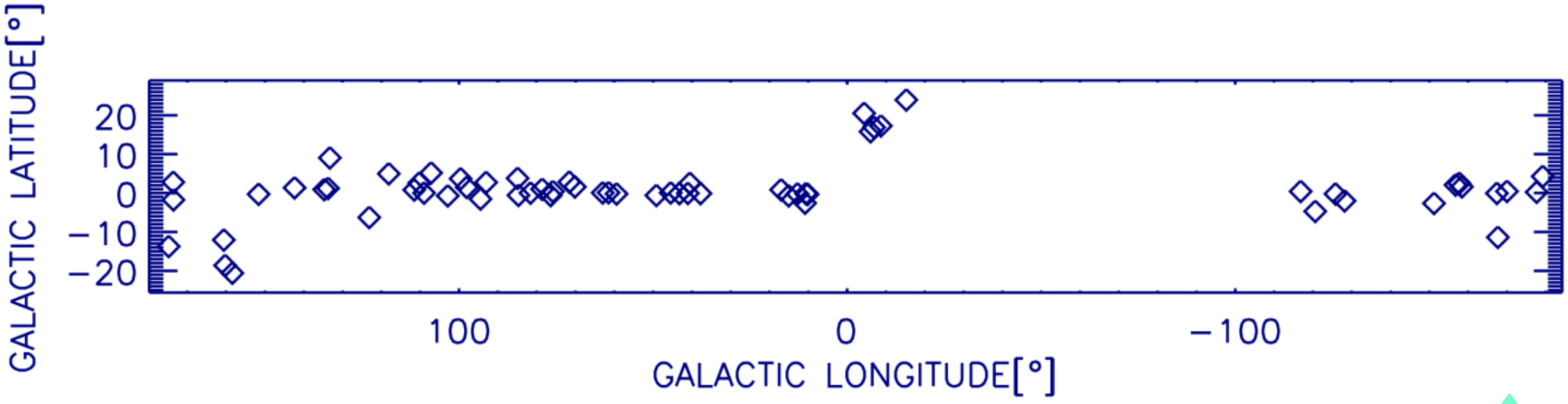

2) QUIJOTE-MFI intensity maps

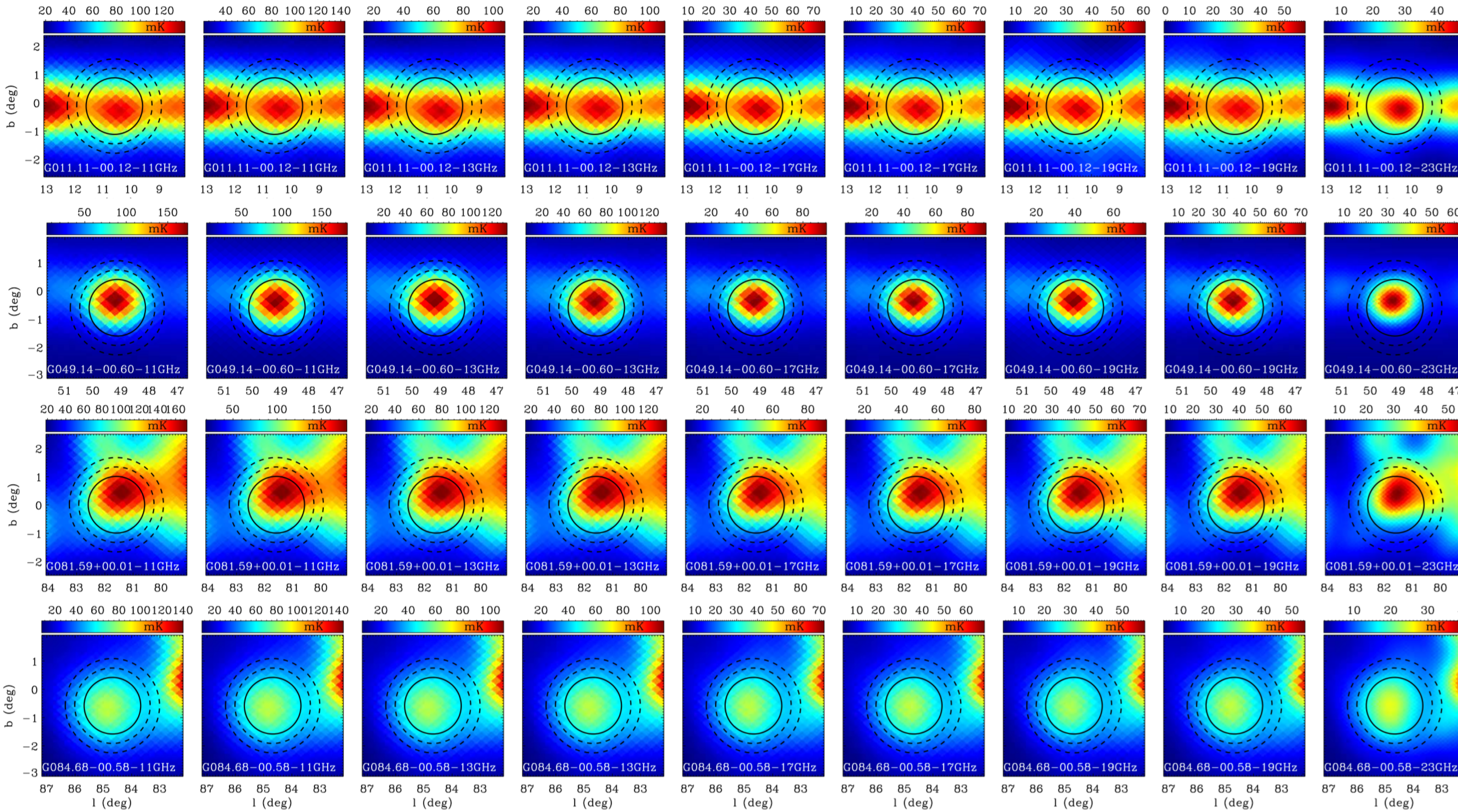

QUIJOTE 11GHz H1 | 11GHz H3 | 13GHz H1 | 13GHz H3 | 17GHz H2 | 17GHz H4 | 19GHz H2 | 19GHz H4 | 22.7GHz WMAP

FROM TOP TO BOTTOM: G011.11-00.12, W51, DR23/DR21 and Dobashi 2743

3) SED Fitting

Free-free, synchrotron, Thermal dust and if needed CMB flux densities are fitted as follow:

$$S_{\mathrm{ff}} = \frac{2\,k\,T_{\mathrm{ff}}\,\Omega\,\nu^2}{c^2}$$

$$S_{\mathrm{sync}} = A_{\mathrm{sync}} \left(\frac{\nu}{\mathrm{GHz}} \right)^{\alpha}$$

$$S_{\mathrm{td}} = 2\,h\,\frac{\nu^3}{c^2}\,\frac{1}{e^{h\nu/kT_{\mathrm{d}}} - 1}\,\tau_{250}\,(\nu/1.2\,\mathrm{THz})^{\beta_{\mathrm{d}}}\,\Omega$$

$$S_{\mathrm{CMB}} = \left(\frac{2\,k\,\Omega\,\nu^2}{c^2} \right) \Delta T_{\mathrm{CMB}}$$

3) SED Fitting

In Planck IR XV (2014) the AME flux densities fit the spinning dust amplitude A_{sp} and the shift frequency $\nu_{\rm shift}$ are fitted as follow:

$$S_{\rm sp} = A_{\rm sp}\, j_{(\nu+\nu_{\rm shift})}\, \Omega$$

where $j(\nu+\nu_{\rm shift})$ is the Warm ISM spinning dust emissivity and ν=28.1 GHz.

In our work the AME flux densities are fitted as in Bonaldi et al. (2007) in the [log(T),log(ν)] space by:

$$\log T_{\rm A,x}(\nu) = {\rm const} - \left[\frac{m_{60}\log\nu_{\rm max}}{\log(\nu_{\rm max}/60\,{\rm GHz})} + 2\right]\log\nu + \frac{m_{60}}{2\log(\nu_{\rm max}/60\,{\rm GHz})}(\log\nu)^2,$$

Quijote

Q-U-I Joint Tenerife CMB experiment

4) SEDs in intensity

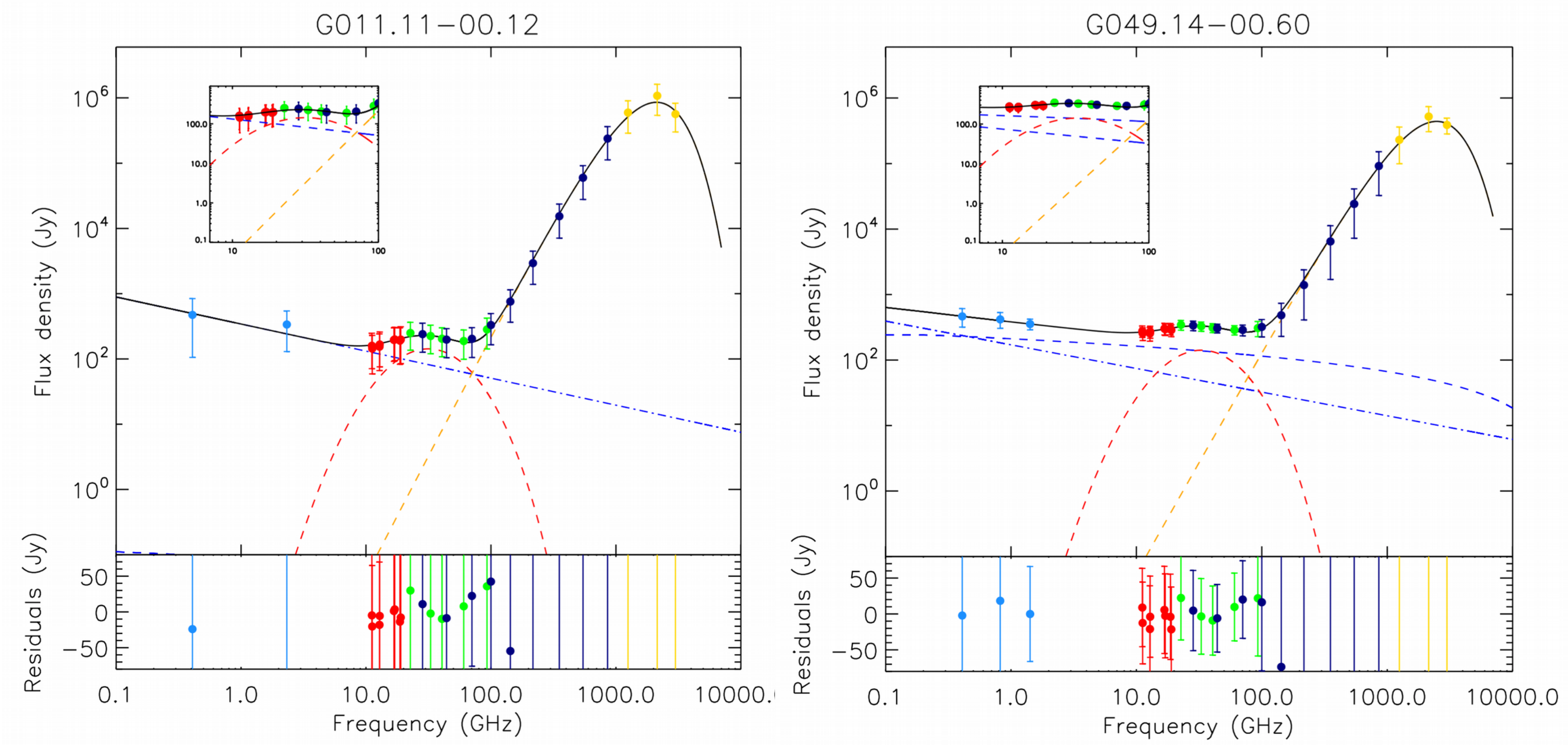

Fitted components: $S_{tot}=S_{ff}+S_{TD}+S_{AME}(AMP_{sp}, m_{60}, \nu_{peak})$

CMB subtracted at map level

4) SEDs in intensity

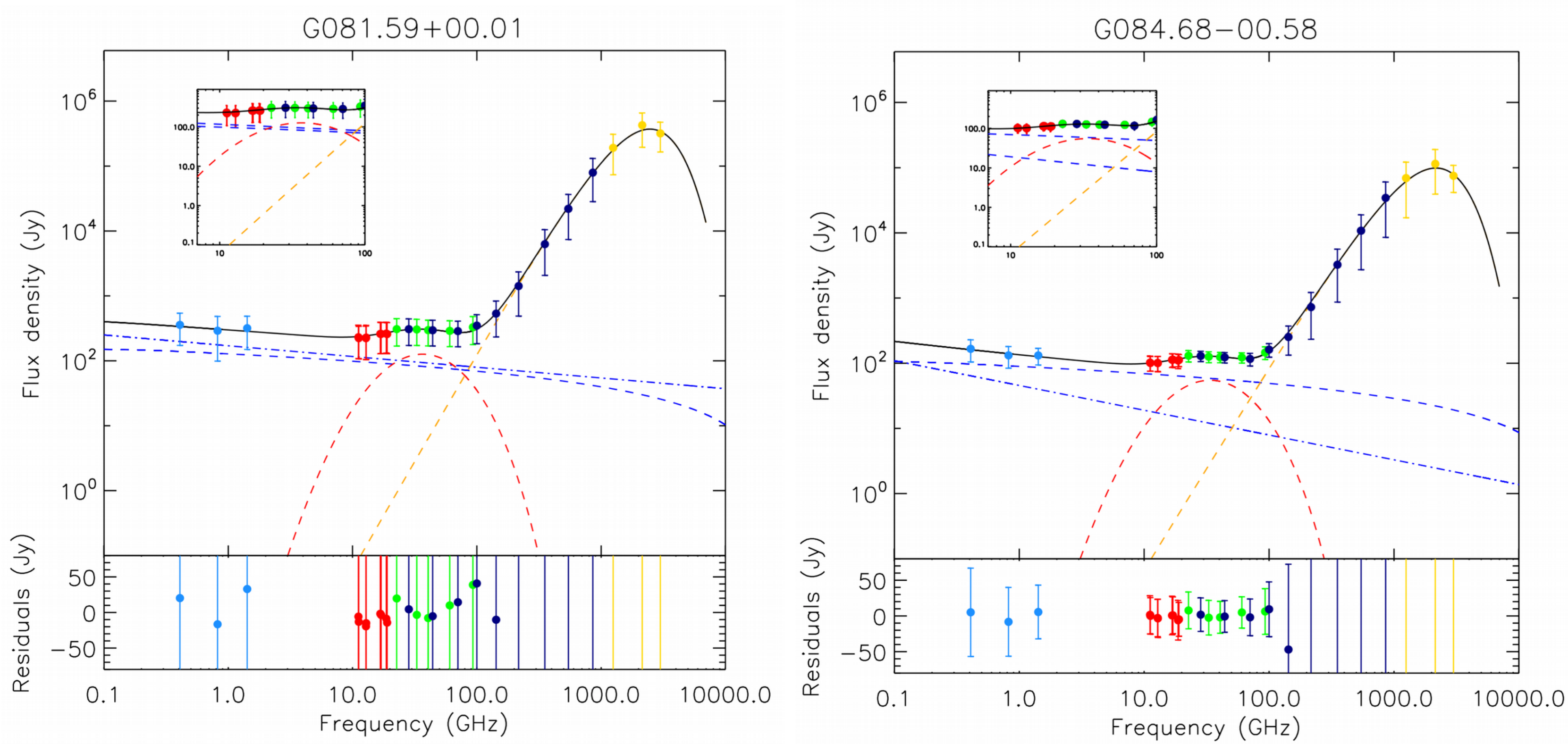

Fitted components: $S_{tot}=S_{ff}+S_{TD}+S_{AME}(AMP_{sp}, m_{60}, \nu_{peak})$

CMB subtracted at map level

5) Comparisons with PIR XV

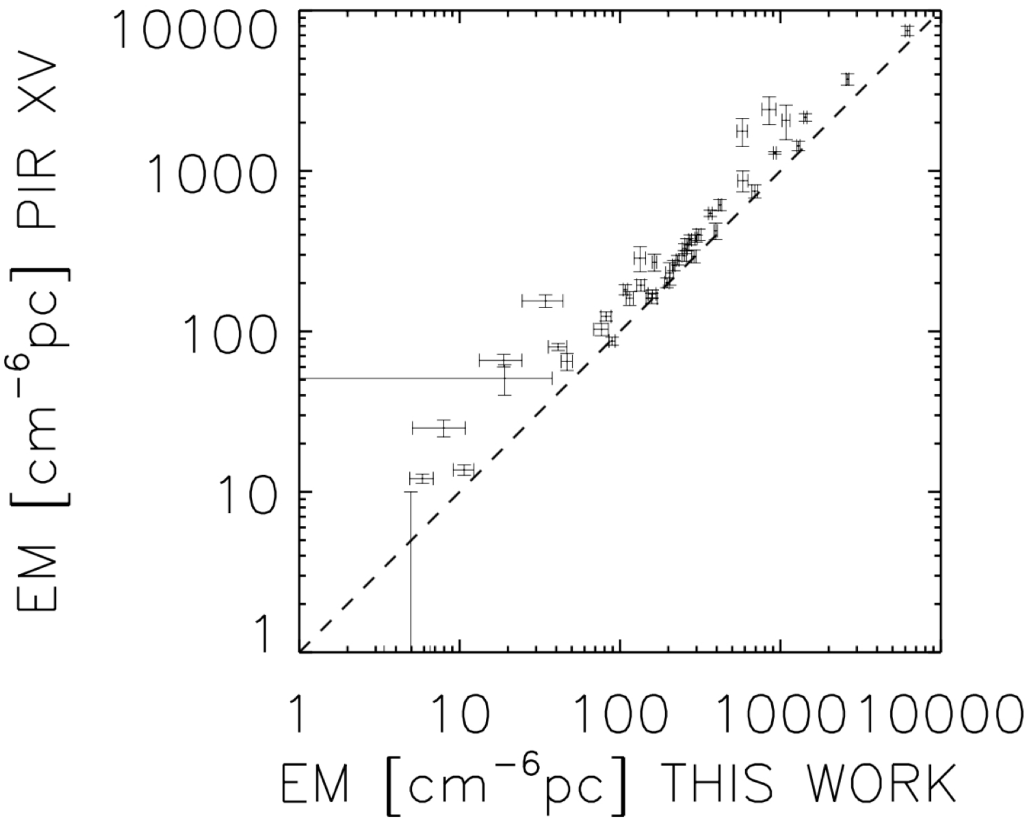

***EM*: Emission Measure of the free-free components**

PIR XV: $S_{tot}=S_{ff}+S_{TD}+S_{\Delta CMB}+S_{AME}(A_{sp},j(\nu+\nu_{shift}))$

This work: $S_{tot}=S_{ff}+S_{TD}+S_{\Delta CMB}+S_{AME}(AMP_{sp},m_{60},\nu_{peak})$

using fixed T_{dust}, β_{dust}, τ_{250}, ΔCMB values from PIR XV

5) Comparisons with PIR XV

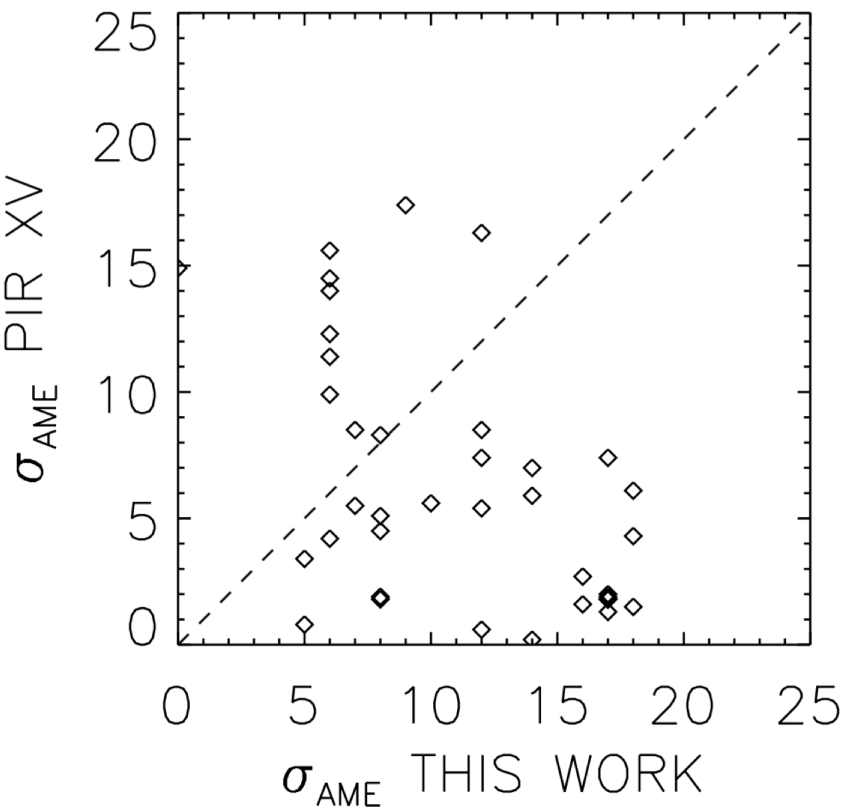

$\sigma_{AME}^{PIR\ XV} = A_{sp}/dA_{sp}$

$\sigma_{AME}^{THIS\ WORK} = AME_{max}/dAME_{max}$

PIR XV: $S_{tot}=S_{ff}+S_{TD}+S_{\Delta CMB}+S_{AME}(A_{sp},j(\nu+\nu_{shift}))$

This work: $S_{tot}=S_{ff}+S_{TD}+S_{\Delta CMB}+S_{AME}(AMP_{sp},m_{60},\nu_{peak})$

using fixed T_{dust}, β_{dust}, τ_{250}, ΔCMB values from PIR XV

5) Comparisons with PIR XV

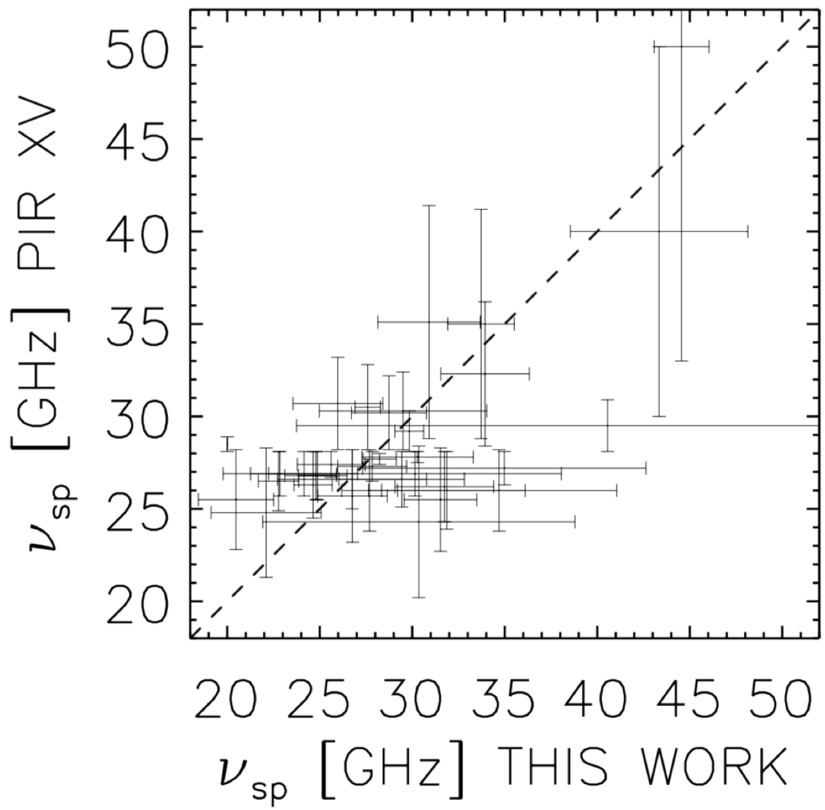

PIR XV: $S_{tot}=S_{ff}+S_{TD}+S_{\Delta CMB}+S_{AME}(A_{sp},j(\nu+\nu_{shift}))$

This work: $S_{tot}=S_{ff}+S_{TD}+S_{\Delta CMB}+S_{AME}(AMP_{sp},m_{60},\nu_{peak})$

using T_{dust}, β_{dust}, τ_{250}, ΔCMB values from PIR XV

5) Comparisons with PIR XV

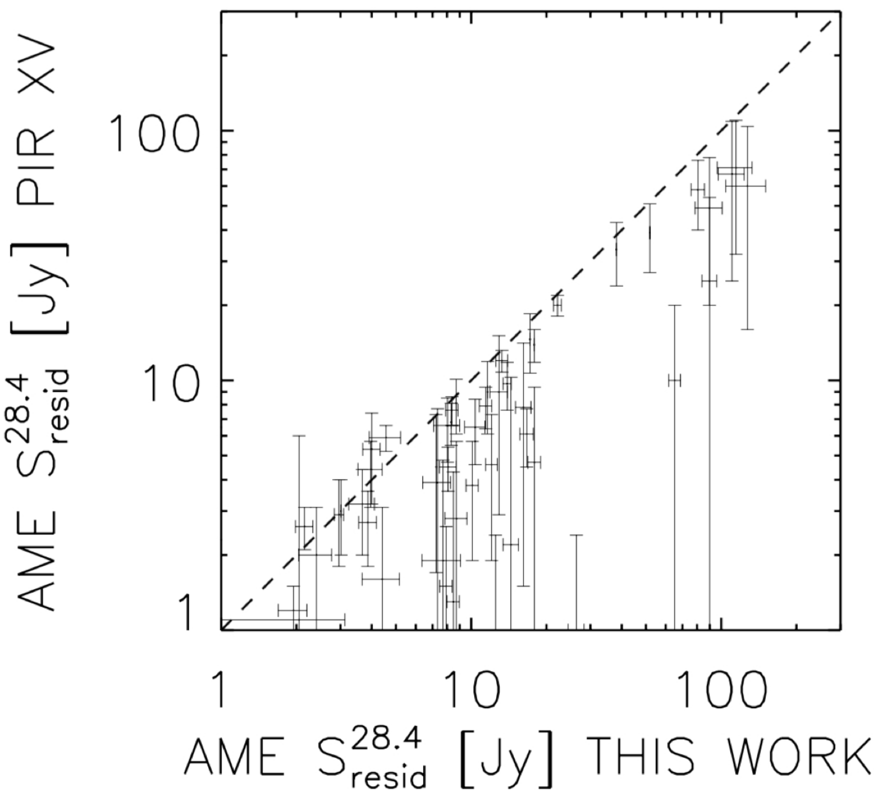

AME $S^{28.4}_{resid} = S_{tot} - S_{ff} - S_{TD} - S_{\Delta CMB}$ at ν=28.4 GHz

PIR XV: $S_{tot}=S_{ff}+S_{TD}+S_{\Delta CMB}+S_{AME}(A_{sp},j(\nu+\nu_{shift}))$

This work: $S_{tot}=S_{ff}+S_{TD}+S_{\Delta CMB}+S_{AME}(AMP_{sp},m_{60},\nu_{peak})$

using fixed T_{dust}, β_{dust}, τ_{250}, ΔCMB values from PIR XV

6) Results

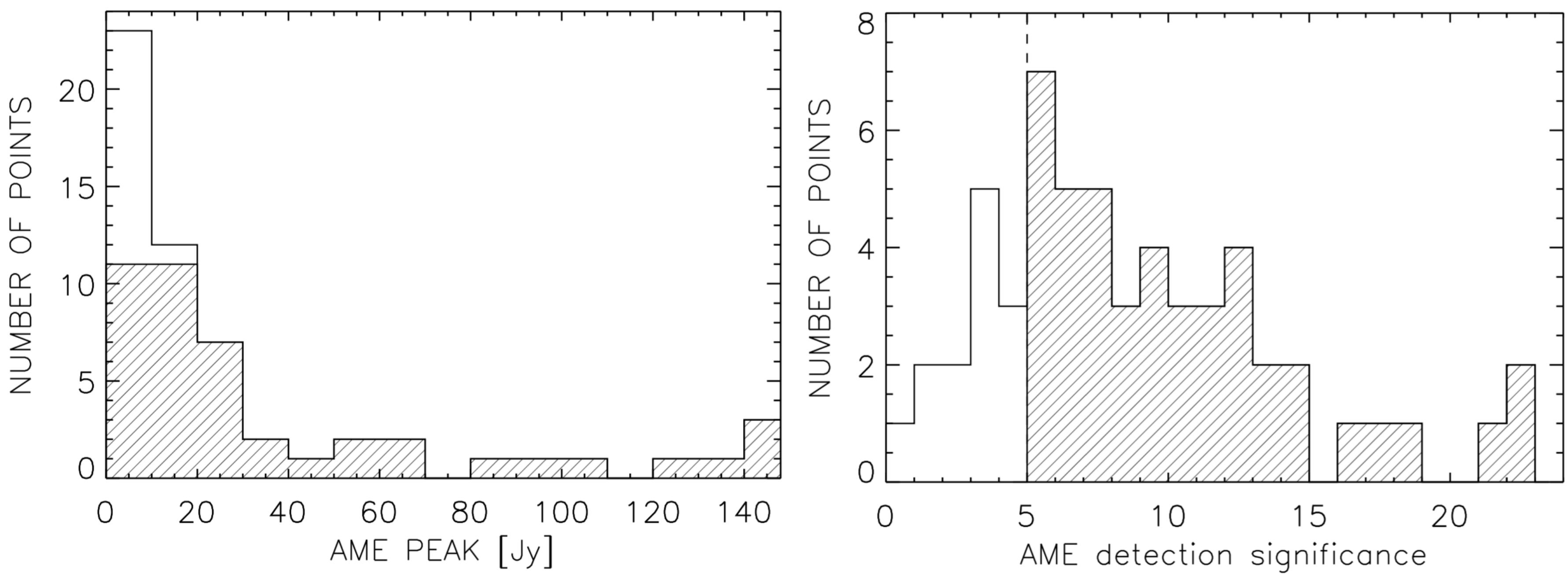

Statistics obtained on the 57/63 effective AME comp.detections

AME detection significance = $AME_{peak}/dAME_{peak}$

44 detections such that $AME_{peak}/dAME_{peak} > 5$

Fitted components: $S_{tot}=S_{ff}+S_{TD}+S_{AME}(AMP_{sp},m_{60},v_{peak})$

CMB subtracted at map level

6) Results

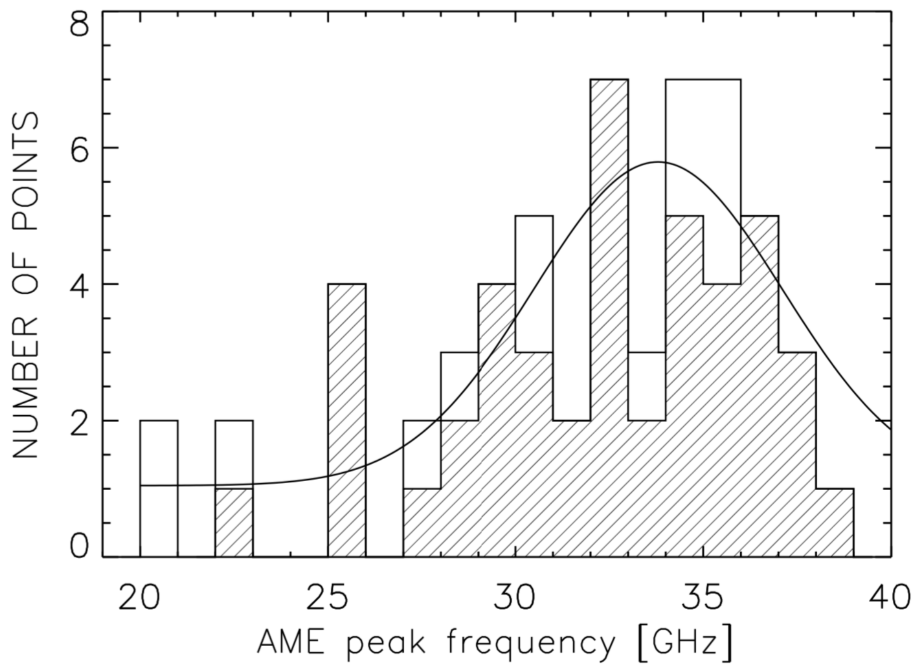

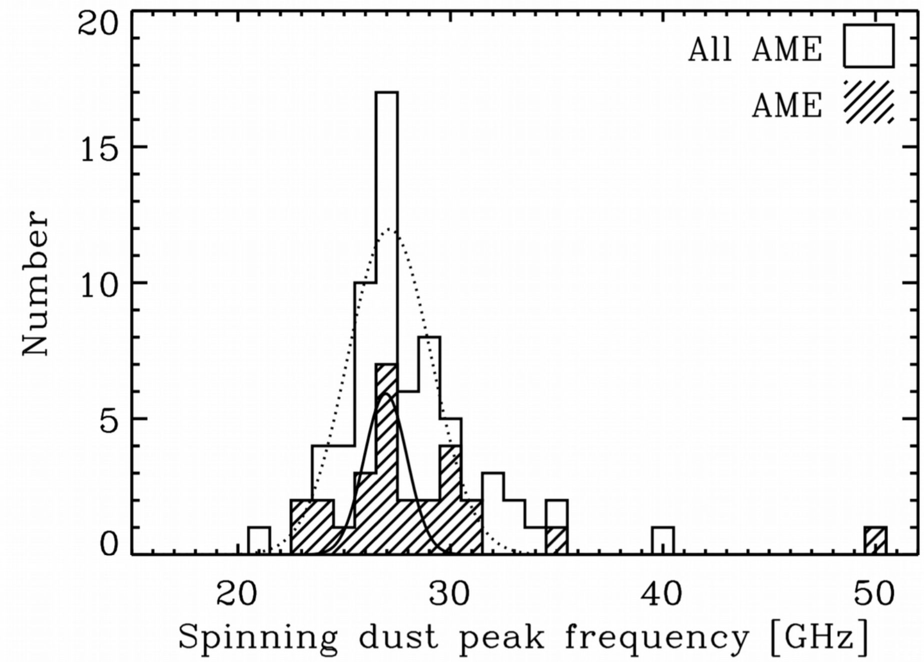

GAUSSIAN FIT TO FULL DATA SET
Peak frequency: **33.8 GHz**
FWHM: 7.8 GHz

PIRXV results for comparisons:
Peak freq:**27.9 GHz**

6) Results

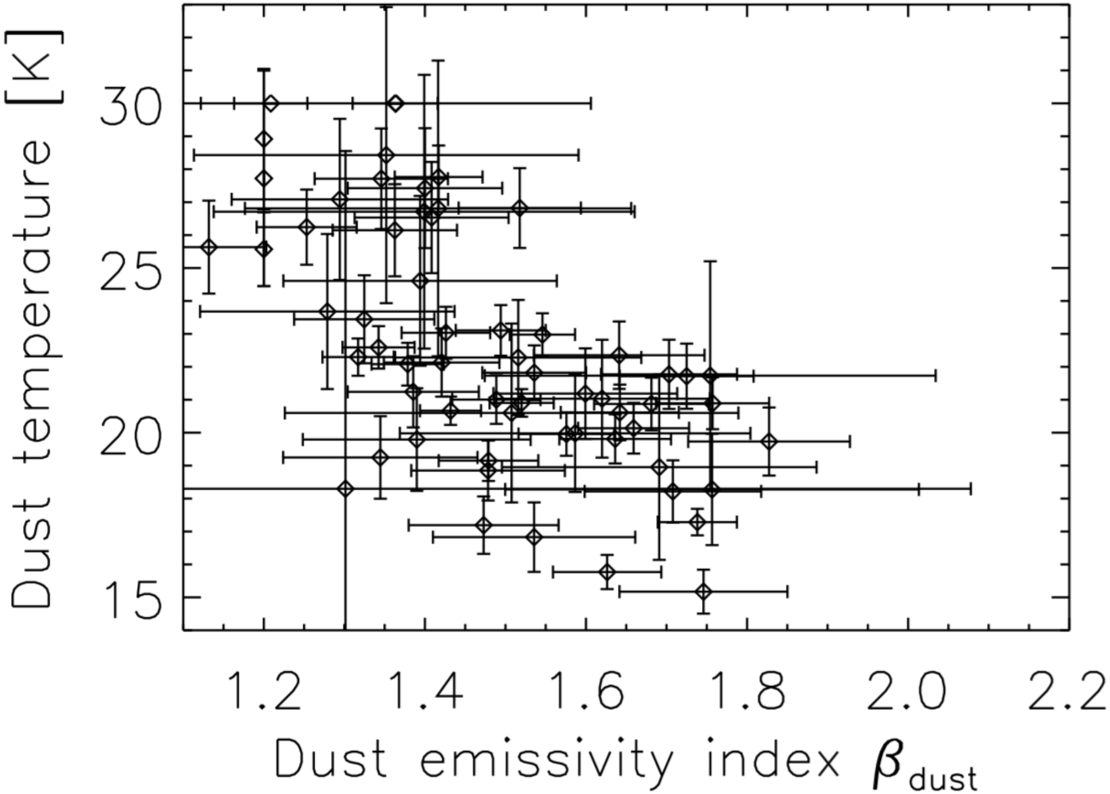

Thermal dust temperature T_{dust} against thermal dust emissivity spectral index β_{dust}

6) Results

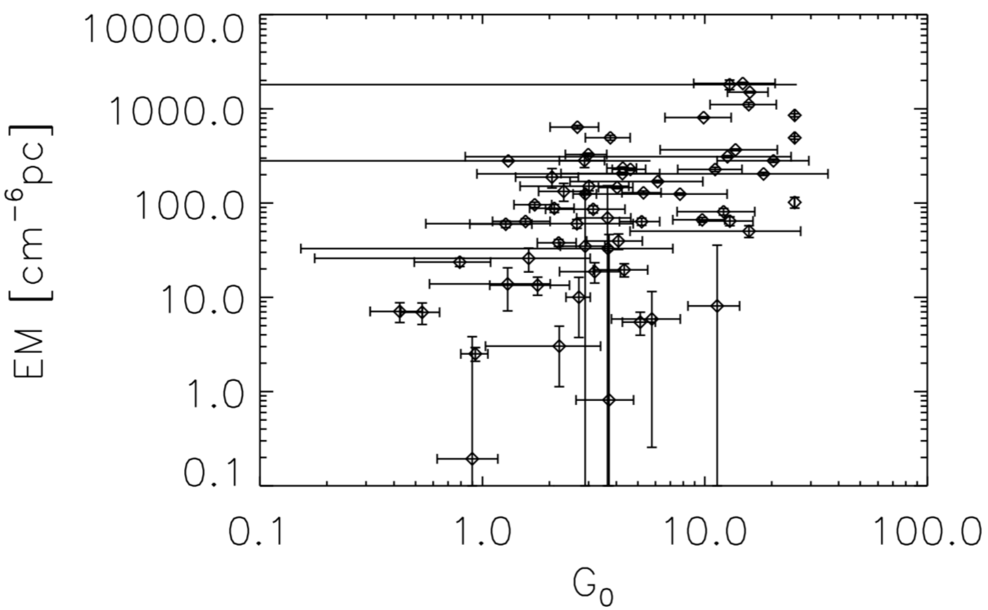

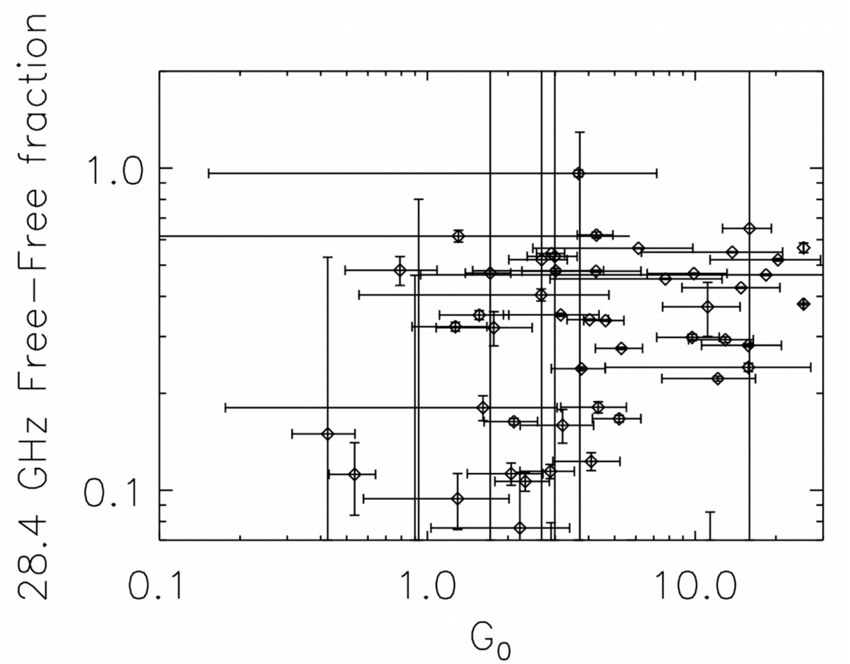

Free-Free Emission Measure (EM) against Interstellar radiation field (G_0)

S_{FF}/S_{TOT} at 28.4GHz against G_0

$G_0 = (T_d/17.5)^{(\beta+4)}$ with T_d = thermal dust temperature [K]
β=2: 'maximum' thermal dust emissivity power-law index

6) Results

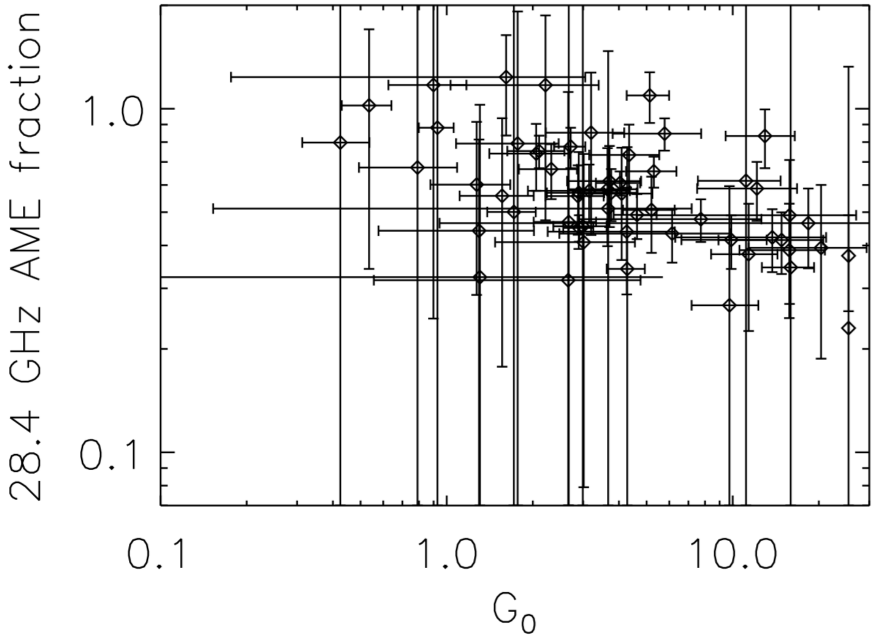

(S_{AME}/S_{TOTAL}) at 28.4GHz against (G_0)

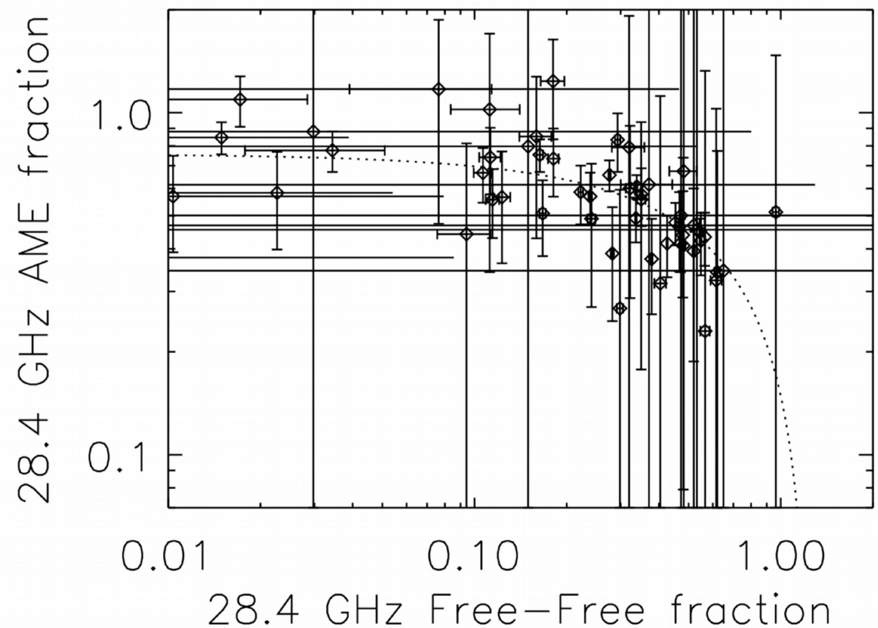

(S_{AME}/S_{TOTAL}) vs (S_{FF}/S_{TOTAL}) at 28.4GHz

$G_0 = (T_d/17.5)^{(\beta+4)}$ where T_d = thermal dust temperature [K]
and β=2: 'maximum' thermal dust emissivity power-law index

(S_{AME}/S_{TOTAL})=-0.6 (S_{FF}/S_{TOTAL}) + 0.76
Spearman rank correlation coefficient: *r_s*=-0.64+\- 7.65e-08

6) Results

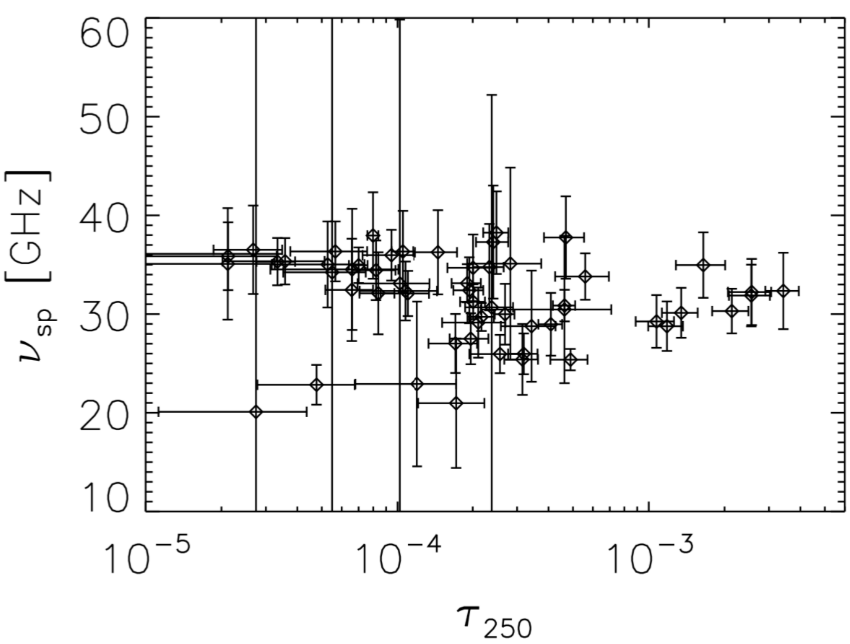

ν_{AME} [GHz] against τ_{250}

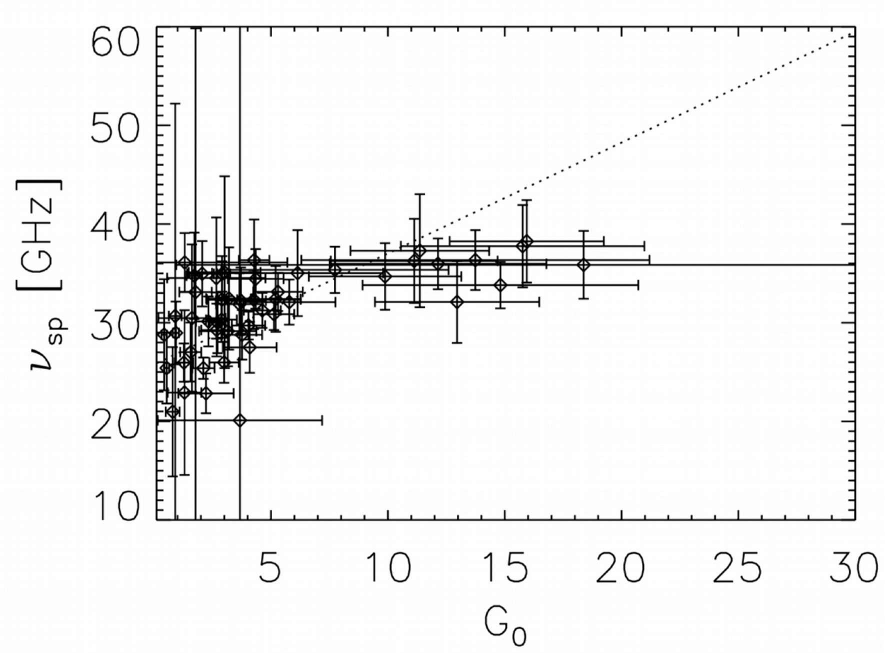

ν_{AME} [GHz] against G_0

ν_{AME}=1.12 G_0 + 25.77

Spearman rank correlation coefficient: r_s=0.61+\- 1.50e-06

Quijote
Q-U-I Joint Tenerife CMB experiment

6) Results

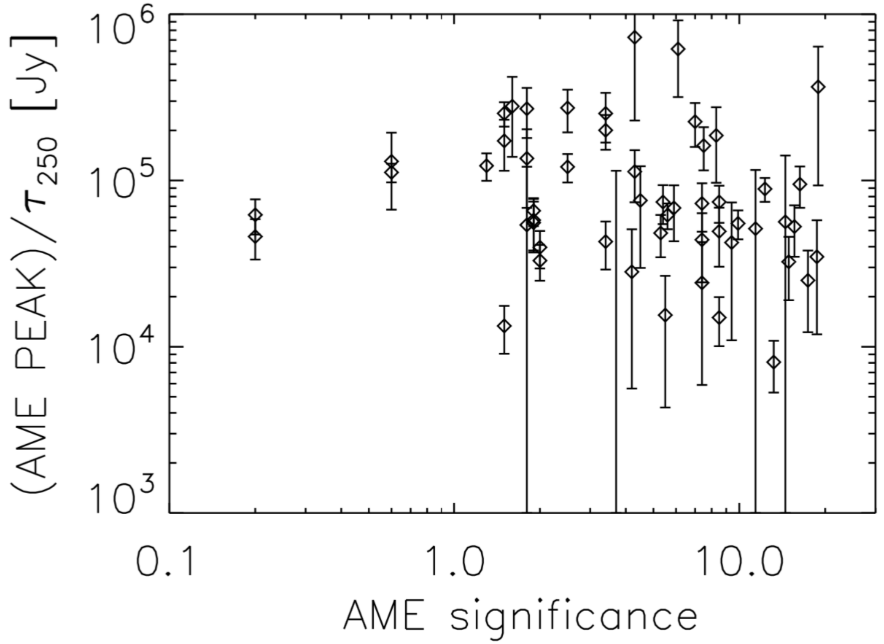

S(AME PEAK)/τ_{250} vs AME significance: S(AME)/dS(AME)

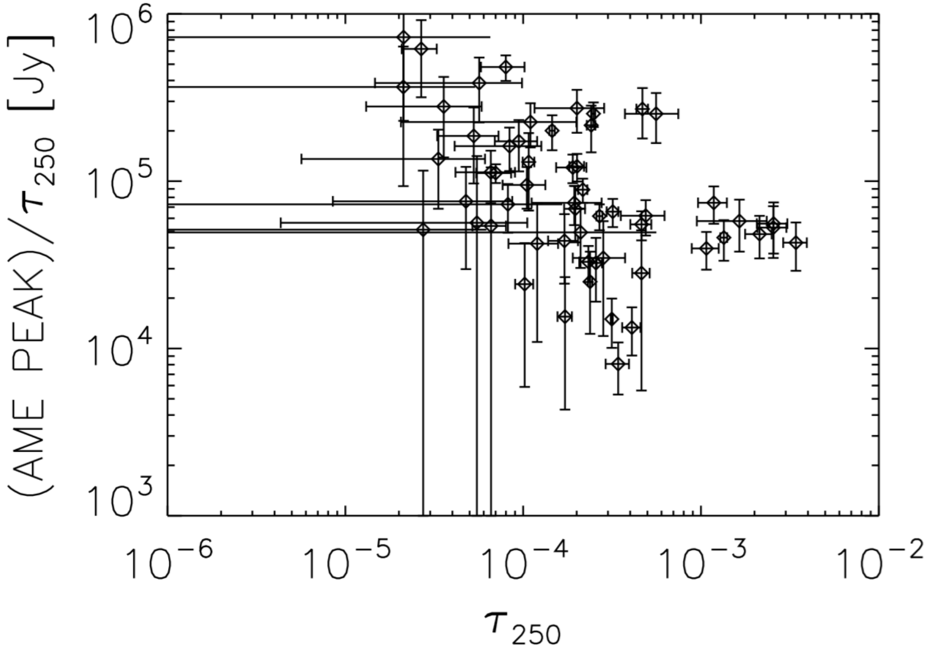

S(AME PEAK)/τ_{250} vs τ_{250}

6) Results

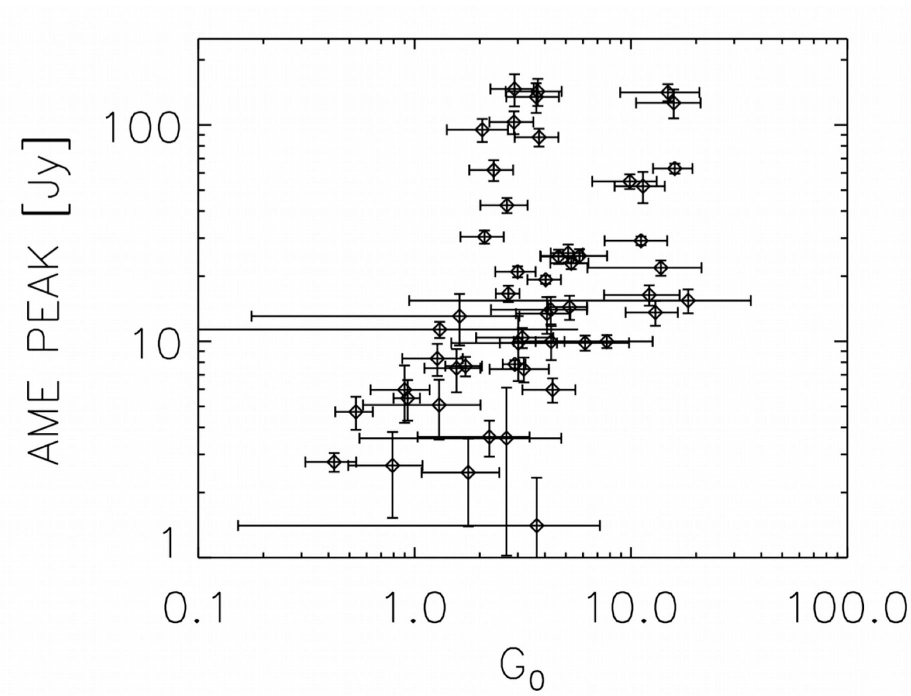

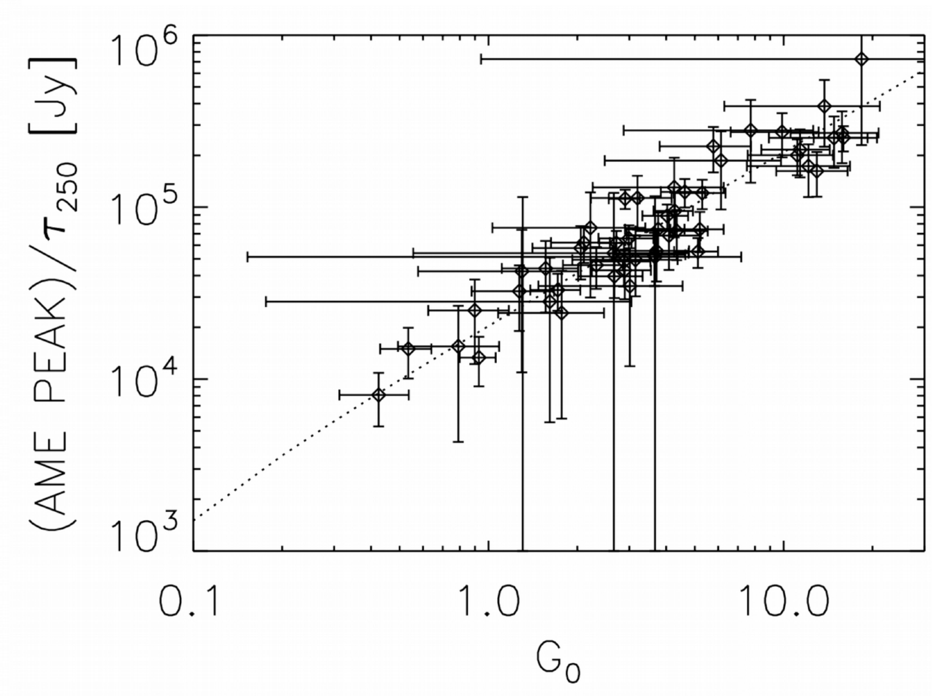

S(AME PEAK) against G_0

S(AME PEAK)/τ_{250} against G_0

$\tau_{250:}$ thermal dust optical depth at 250 μm

S(AME PEAK)/τ_{250}=20919.5 G_0 - 591.4

Spearman rank correlation coefficient: *r_s*=0.91+\- 2.37e-20

6) Results

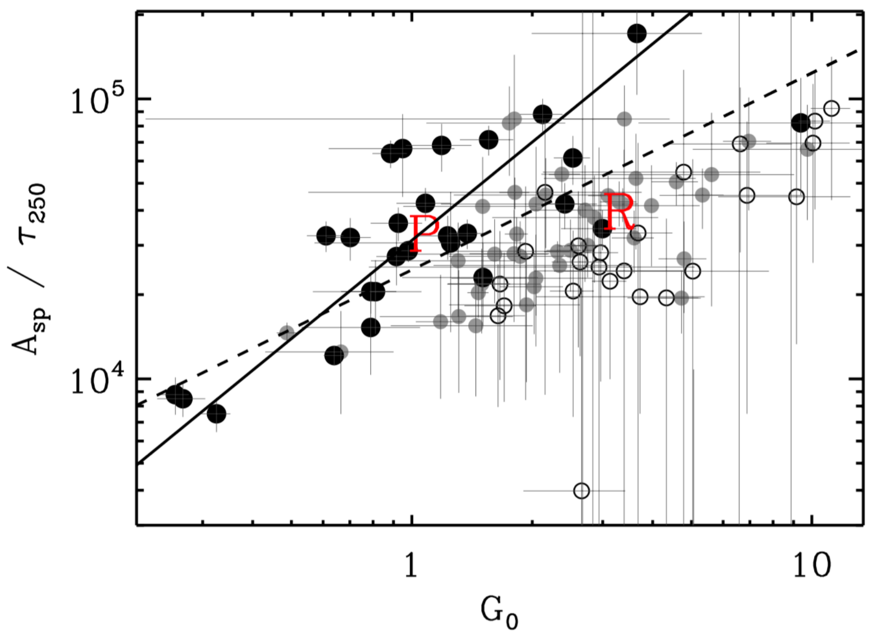

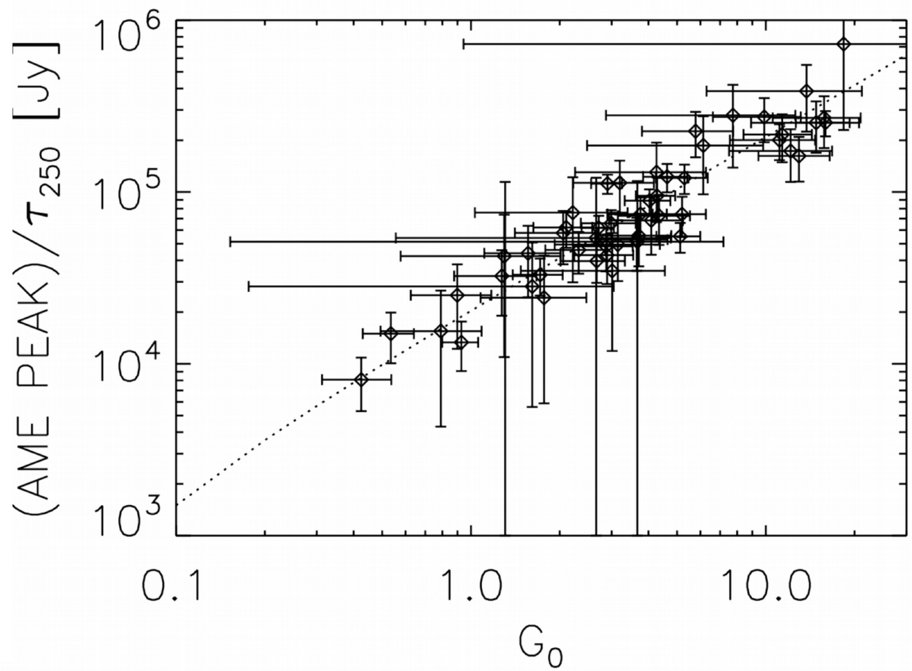

Asp/τ_{250} against G_0 (PIR XV)

The straight lines are the best-fitting power laws to the AME (solid line) and including semi-significant AME (dashed line) regions.

S(AME PEAK)/τ_{250} against G_0

Results obtained in PIR XV (left figure) do not show clear trend as results obtained fromOur analysis (right).

→ Possible contamination by UCHII regions has to be included in our analysis but should not change observed correlation

7) Summary

- Total of 63 candidate AME sources (51 discussed in PIR XV)
- The QUIJOTE-MFI maps improve the detection of AME in most sources:

    - Lower estimations of Free-Free than in PIR XV

    - Higher estimates of *S*(AME PEAK) at 28.4 GHz than in PIRXV

- AME components fitted by Bonaldi model
- 44 detections such that S(AME)/dS(AME) > 5
- Strong correlation between S(AME PEAK)/τ_{250} and G_0
- Correlation between ν_{AME} [GHz] and G_0


Thank you!
2016/02/22
Carlos MR